

Spontaneous Resolution of a Mixed-Ligand Nickel(II) Coordination Polymer with Achiral Precursors

Kamal Kumar Bisht and Eringathodi Suresh*

Analytical Discipline and Centralized Instrument Facility, Central Salt and Marine Chemicals Research Institute, Council of Scientific and Industrial Research (CSIR), G. B. Marg, Bhavnagar 364 002, Gujarat, India

Supporting Information

ABSTRACT: Metal-center-driven spontaneous resolution of a chiral coordination polymer, $[\text{Ni}(\text{SDB})(\text{BIX})]_n$ (**1**), from achiral precursors has been probed by single-crystal X-ray diffraction and circular dichroism spectroscopy. Enantiomorphs **1P** and **1M** showed a parallel interpenetrated 2D \rightarrow 3D chiral framework with $(8^2.10)$ topology. Switching of the metal center under the same reaction parameters resulted in isostructural achiral and noninterpenetrating (4,4) grid-type **sql** networks $[\text{M}(\text{SDB})(\text{BIX})]_n$, where $\text{M} = \text{Co}^{\text{II}}$, Zn^{II} , and Cd^{II} for **2–4**, respectively.

Chirality possesses a distinguished place in nature and plays an important role in biological and material sciences. Chiral supramolecular assemblies, specifically chiral coordination polymers (CPs), are receiving immense attention in recent years because of their fundamental importance in the area of asymmetric catalysis and chiral recognition.¹ Achieving homochirality in CPs has been a challenging task, and there are three prime methodologies to construct homochiral CPs: (a) the use of an enantiopure organic ligand, which translates chirality to the resultant framework by a “chirality conservation” process; (b) the use of chiral auxiliaries such as an enantiopure solvent, additive, catalyst, or template, which may “induce” chirality; (c) by means of crystallization without using any enantiopure substance, which results in the chiral spatial arrangements of metal and achiral ligands. All of these methodologies are comprehensively described and demonstrated in the literature.^{2,3} The spontaneous resolution of CPs from achiral precursors usually results in conglomerates, i.e., a mixture of homochiral crystals having opposite handedness. Various factors such as coordination around the metal center, flexibility of the ligands, and inter/intramolecular hydrogen-bonding and stacking interactions can maneuver the formation of chiral CPs from achiral building blocks. The homochiral crystallization of CPs from achiral building blocks is a scanty explored area.³ In addition to the chirality, the topology of CPs also plays a crucial role in determining the inherent properties of the material.⁴ There are not many reports on mere the switching of the metal center resulting in significant topological or structural contrasts under identical reaction conditions. Recently, Hupp et al. have reported two metal–organic frameworks (MOFs) with **rht** topology, where significant structural differences were achieved by the switching of metal centers.⁵

Herein, we report the spontaneous resolution of a CP conglomerate, $[\text{Ni}(\text{SDB})(\text{BIX})]_n$ (**1**), comprising of Ni^{II} centers helically connected by flexible ligand **BIX** [1,4-bis(imidazol-1-ylmethyl)benzene] and angular ligand **SDB** (4,4'-sulfonyldibenzoate). Both enantiomeric forms **1P** and **1M** are established by single-crystal X-ray diffraction (XRD) and solid-state circular dichroism (CD) spectroscopy. We also report three achiral and isostructural CPs, **2–4**, constructed by switching the metal node of **1** from Ni^{II} to Co^{II} , Zn^{II} , and Cd^{II} , respectively, under the same solvothermal reaction conditions. The photoluminescence properties of all of the CPs **1–4** have also been explored.

Compounds **1–4** were synthesized solvothermally by treating the metal salts, H_2SDB and **BIX** at 125 °C and were characterized by Fourier transform infrared spectroscopy, thermogravimetric analysis (TGA), and powder XRD (PXRD; Figures S1–S4 in the Supporting Information, SI). The bulk purity and thermal stability of all of the compounds were ascertained by PXRD and TGA. Compounds **1–4** liberate their lattice guests in the temperature range 120–180 °C and are fairly stable up to ca. 280 °C.

During crystallization, spontaneous resolution occurs and the single crystals of both enantiomorphs of **1** (**1P** and **1M**) have been randomly selected under a polarized microscope. The X-ray crystallographic studies revealed that **1P** and **1M** are enantiomorphs, and henceforth the structure of **1P** is discussed in detail. Both crystals **1P** and **1M** crystallized in the orthorhombic system with chiral space group $F222$. The asymmetric unit of **1P** contains half of a Ni^{II} cation, occupying a special position and C_2 symmetry; half of **BIX**, and half of a **SDB** anion, each lying on an independent C_2 axis bisecting the central phenyl ring and passing through the S atom, respectively. Four carboxylate O atoms (in chelated form) from two **SDB** anions and two N atoms from two **BIX** ligands provide the distorted octahedral geometry around Ni^{2+} (Figure 1).

The symmetrically disposed N atom and chelated carboxylate O atom from different **BIX** and **SDB** moieties in *cis* coordination constitute the square base in **1P**. The crystal structure revealed a 2D CP with P and M helical patterns in **1P** and **1M**, respectively. The structure of **1** can best be described as follows: $[\text{Ni}_2(\text{BIX})_2]$ dimeric units (Figure S9 in the SI), in which the **BIX** moieties adopt a gauche conformation, are intertwined and bridge the metal centers with a $\text{Ni}\cdots\text{Ni}$

Received: July 26, 2012

Published: August 31, 2012

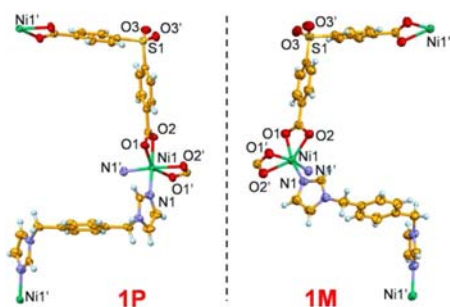


Figure 1. Coordination environment around the Ni^{II} ions in enantiomorphs **1P** and **1M**.

separation of 12.11 Å. [Ni₂(BIX)₂] dimeric units are oriented along the *b* axis and down the *a* axis, with the Ni cations from different stacked dimeric units encompassing a 2₁ screw orientation down the *a* axis. Layers of dimeric units stacked down the *a* axis and along the *c* axis are coupled through the terminal carboxylate O atoms from two SDB ligands.

Screw-related Ni^{II} ions of the neighboring units (along the *c* axis and down the *a* axis) are linked alternatively (“up” and “down” manner) by the chelated carboxylate O atoms of SDB, generating a 2D network imparting right- (**P**) and left-handed (**M**) helicities for **1P** and **1M**, respectively (Figures 2 and S8–

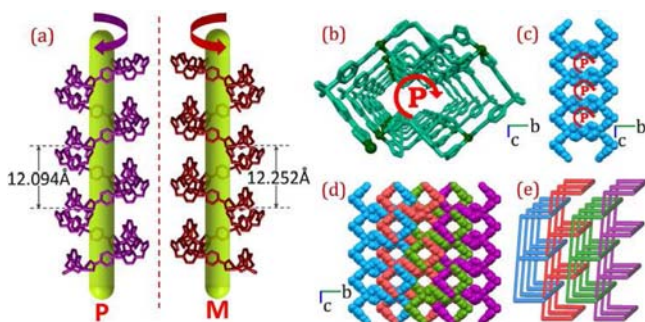


Figure 2. (a) **P** and **M** helical motifs running down the *a* axis in **1P** and **1M**, respectively. (b) Top view of a **P** helix. (c) **P** helices fused together to construct 2D sheets. (d) 2D sheets undergo 2D → 3D parallel interpenetration. (e) Topological depiction of **1P** and **1M** (the helical pitch is 12.09 Å in **1P** 12.52 Å in **1M**).

S10 in the SI). The Ni⋯Ni separation distance bridged by the bent SDB ligands with pairs of Ni₂(BIX)₂ units is 13.16 Å. The chelated coordination of carboxylate groups imparts severe strain in the octahedral Δ and Λ configurations around the metal centers in **1P** and **1M**, respectively (Figures 1 and S8 in the SI). The spatial arrangements of flexible BIX and SDB ligands reveal that the average dihedral angles between the two peripheral imidazole rings are 55.6° and 55.1° in BIX and those between the aryl rings are 81.1° and 78.5° in the case of SDB in **1P** and **1M**, respectively, indicating severe twist in these ligands to make an effective coordination with the metal. Overall, the spontaneous resolution of chiral MOFs may be attributed to the coordination geometry around Ni²⁺ and the spatial orientation of the flexible ligands. **1P** and **1M** exhibited three connected uninodal topologies described by a short vertex symbol (8².10). Interestingly, the 2D sheets are further involved in 3-fold interpenetration to realize a rare 2D → 3D parallel polycatenated network, as depicted in Figure 2e. The polycatenated nets are stabilized via intermolecular C–H⋯O interactions between the carboxylate atoms O1 and O2 with

H8 and H11A of the BIX ligand. Each Ni atom is connected to three other Ni atoms by means of two BIX and two SDB moieties, yielding a three-connected node (3c). These 3c nodes form a thick 2D (8².10) net extending along the *ac* plane. The sufficient thicknesses of these nets allow 3-fold parallel interpenetration in one “above” and one “below” fashion that results in the extension of the structure in third dimensions, i.e., along the *b* axis. It is worth mentioning here that the achiral isomer of **1** has recently been reported by Liu and co-workers.⁶

The chiral nature of the enantiomorphs **1P** and **1M** was established by solid-state CD spectra of the same single crystal that was solved as **1P** by XRD. As depicted in Figure 3, **1P**

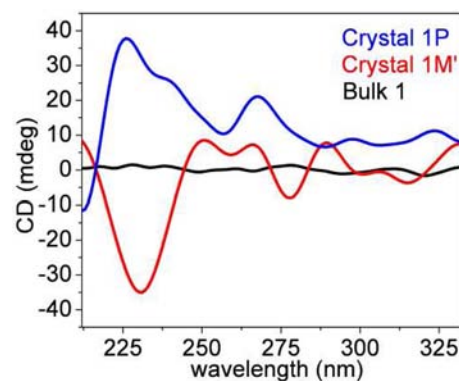


Figure 3. Solid-state CD spectra of **1P**, an enantiomorphic crystal (**1M'**), and a mixture of a few crystals.

exhibits a positive dichroic signal at 215–250 nm (electronic absorption region of **1**; Figure S5 in the SI), which may be considered as the signature of the **P** helicity and Δ configuration. Another crystal showed an enantiomeric CD signal corresponding to **1M** (Figure 3). Additionally, four of nine randomly selected single crystals exhibit positive CD signals, and the remaining five showed negative CD signals, while a mixture of a few crystals did not show dichroic signals (Figure S7 in the SI). Concurrence of the CD experiments and single-crystal studies confirms that **1** is a conglomerate consisting of enantiomorphs **1P** and **1M**.

Replacement of Ni^{II} with Co^{II}, Zn^{II}, and Cd^{II} yielded isostructural achiral CPs **2–4** with (4,4) grid networks, and the structural description is limited to **2** (Figures S11–S13 in the SI). The asymmetric unit of **2** contains one Co²⁺ center, one SDB dianion, and half a molecule of the BIX ligand with an inversion center at the midpoint of the central phenyl ring. Pairs of Co^{II} ions are joined by four symmetrically disposed SDB ligands in the syn–syn mode to generate a dinuclear Co^{II} “paddlewheel”-type secondary building unit (SBU) with a Co⋯Co distance of 2.856(4) Å. These paddlewheel SBUs are connected via a second carboxylate group of the symmetrical SDB dianions into a 1D double chain along the *a* axis with a Co⋯Co distance of 12.88 Å. The metal centers of the dimeric double-chain loops are pillared (along the *c* axis) by the N atom of the BIX ligand axially (Co⋯Co distance of 14.50 Å), generating a 2D (4,4) grid-type sq1 network (Figures 4 and S14 in the SI). M²⁺ possesses a square-pyramidal geometry provided by four carboxylate O atoms from SDB, forming the square base and axial coordination from the imidazole atom N1. The imidazole rings of BIX in the anti conformation pillaring the dimeric double chain are parallel to each other, whereas the phenyl rings of the SDB ligand are almost perpendicular

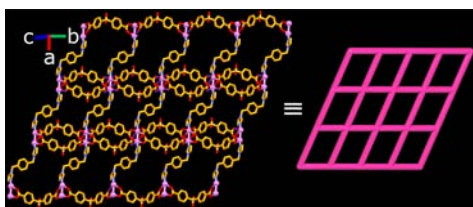


Figure 4. Structural and topological depiction of the (4,4) net in **2** showing the $\text{Co}_2(\text{SDB})_2$ chains axially connected by BIX moieties.

(82.9°). A comparison of these dihedral angles with **1P** shows the severe twist for BIX terminal imidazole rings in **1P** (55.6°).

Considering the previous reports on the photoluminescence properties of CPs derived from the H_2SDB or BIX ligand, the luminescent behavior of **1–4** has been examined at room temperature.⁷ As illustrated in Figure 5, the free ligands H_2SDB

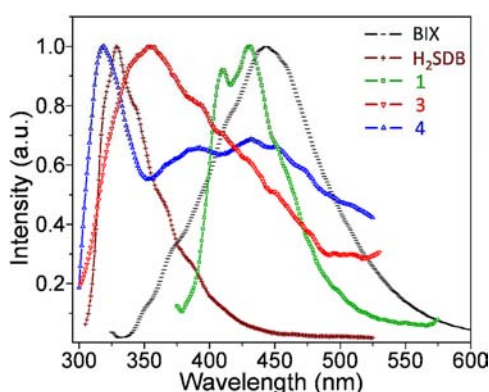


Figure 5. Solid-state luminescence spectra of ligands and CPs **1**, **3**, and **4** recorded at room temperature.

and BIX exhibit strong fluorescence bands at 329 nm ($\lambda_{\text{ex}} = 295$ nm) and 443 nm ($\lambda_{\text{ex}} = 317$ nm), respectively (ascribed to $\pi^* \rightarrow \pi$ and $\pi^* \rightarrow n$ transitions). Generally, the CPs containing d_{10} metal ions like Zn^{II} and Cd^{II} show strong fluorescence and those containing Ni^{II} and Co^{II} barely fluoresce. Interestingly, **1** shows strong emission bands at 410 and 431 nm when excited at 350 nm in the vicinity of free BIX emission, and this may be attributed to the intraligand transitions of the robust intertwined dimeric BIX motif realized in **1**.⁸ Upon excitation at 325 nm, **2** exhibits a weak fluorescence band at 414 nm (Figure S6 in the SI). CPs **3** and **4** exhibit intense fluorescence at 355 nm ($\lambda_{\text{ex}} = 289$ nm) and 319 nm ($\lambda_{\text{ex}} = 289$ nm), respectively, which may be attributed to the metal-perturbed intraligand emission of SDB involved in rigid paddlewheel motifs. A red shift of 26 nm for **3** and a blue shift of 10 nm for **4** may be accounted for to the extent of metal–ligand coordination and the different sizes of the metal ions. Additional humps at 392 and 432 nm for **4** are ascribed to the metal to ligand–intraligand charge transfers of BIX.⁹

In summary, the spontaneous resolution of a CP, $[\text{Ni}(\text{SDB})(\text{BIX})]_n$, in two enantiomorphs, **1P** and **1M**, has been unambiguously established by crystallography and CD spectroscopy. Chirality in **1P** and **1M** is induced by the self-assembly of homochiral helical motifs driven by coordination around the metal center, ligand flexibility, and hydrogen-bonding interactions. Under identical reaction conditions, Co^{II} , Zn^{II} , and Cd^{II} metal salts resulted in isostructural (4,4) grid-type **sql** networks. CPs **1**, **3**, and **4** show strong photoluminescence originating from the ligands and robust metal–

organic motifs, particularly the $\text{Ni}_2(\text{BIX})_2$ motif in **1** and paddlewheel SBUs in **3** and **4**. The present study highlights the collective role of metal coordination geometry and ligand flexibility in the molecular self-assembly of homochiral CPs from achiral ligands. Acquiring insight from the present results, we are currently exploring the design and synthesis of chiral CPs from more flexible achiral ligands.

■ ASSOCIATED CONTENT

■ Supporting Information

Experimental details, CIF files, Figures S1–S15, and Tables S1–S3. This material is available free of charge via the Internet at <http://pubs.acs.org>.

■ AUTHOR INFORMATION

Corresponding Author

*E-mail: esuresh@csmcricri.org or sureshe123@rediffmail.com.

Notes

The authors declare no competing financial interest.

■ ACKNOWLEDGMENTS

Authors acknowledge the CSIR, India (Grant NWP-0010), for financial support, Dr. P. Bhatt for PXRD data, S. N. Patel for TGA data, V. K. Agrawal for IR data, and Dr. P. Paul for all-around analytical support. K.K.B. acknowledges the CSIR (India) for SRF.

■ REFERENCES

- (1) (a) Davis, M. E. *Nature* **2002**, *417*, 813. (b) Kesanli, B.; Lin, W. *Coord. Chem. Rev.* **2003**, *246*, 305. (c) Pérez-García, L.; Amabilino, D. B. *Chem. Soc. Rev.* **2002**, *31*, 342. (d) Song, Y. M.; Zhou, T.; Wang, X. S.; Li, X. N.; Xiong, R. G. *Cryst. Growth Des.* **2006**, *6*, 14–17. (e) Suh, K.; Yutkin, M. P.; Dybtsev, D. N.; Fedin, V. P.; Kimoon Kim, K. *Chem. Commun.* **2012**, *48*, 513–515.
- (2) (a) Zhang, J.; Liu, R.; Feng, P.; Bu, X. *Angew. Chem., Int. Ed.* **2007**, *46*, 8388–8391. (b) Lin, Z.; Slawin, A. M. Z.; Morris, R. E. *J. Am. Chem. Soc.* **2007**, *129*, 4880–4881. (c) Gao, E. Q.; Yue, Y. F.; Bai, S. Q.; He, Z.; Yan, C. H. *J. Am. Chem. Soc.* **2004**, *126*, 1419–1429.
- (3) (a) Zhang, J.; Chen, S.; Wu, T.; Feng, P.; Bu, X. *J. Am. Chem. Soc.* **2008**, *130*, 12882–12883. (b) Ou, G. C.; Jiang, L.; Feng, X. L.; Lu, T. B. *Inorg. Chem.* **2008**, *47*, 2710–2718. (c) Tong, X. L.; Hu, T. L.; Zhao, J. P.; Wang, Y. K.; Zhang, H.; Bu, X. H. *Chem. Commun.* **2010**, *46*, 8543–8545. (d) Zheng, X. D.; Zhang, M.; Jiang, L.; Lu, T. B. *Dalton Trans.* **2012**, *41*, 1786.
- (4) (a) Batten, S. R.; Robson, R. *Angew. Chem., Int. Ed.* **1998**, *37*, 1460–1494. (b) Carlucci, L.; Ciani, G.; Proserpio, D. M. *Coord. Chem. Rev.* **2003**, *246*, 247–289.
- (5) Hupp, J. T. *Cryst. Growth Des.* **2012**, *12*, 1075–1080.
- (6) Liu, G. X.; Xu, H.; Zhou, H.; Nishihara, S.; Ren, X. M. *CrystEngComm* **2012**, *14*, 1856.
- (7) (a) Hu, M. H.; Shen, G. L.; Zhang, J. X.; Yin, Y. G.; Li, D. *Cryst. Growth Des.* **2009**, *9*, 4533–4537. (b) Xiao, D. R.; Li, Y. G.; Wang, E. B.; Fan, L. L.; An, H. Y.; Su, Z. M.; Xu, L. *Inorg. Chem.* **2007**, *46*, 4158–4166. (c) Liu, G. X.; Zhu, K.; Xu, H. M.; Nishihara, S.; Huang, R. Y.; Ren, X. M. *CrystEngComm* **2009**, *11*, 2784–2796.
- (8) (a) Valeur, B. *Molecular Fluorescence: Principles and Applications*; Wiley-VCH: Weinheim, Germany, 2002. (b) Zheng, S. L.; Yang, J. H.; Yu, X. L.; Chen, X. M.; Wong, W. T. *Inorg. Chem.* **2004**, *43*, 830–838.
- (9) (a) Chen, X. L.; Gou, L.; Hu, H. M.; Fu, F.; Han, Z. X.; Shu, H. M.; Yang, M. L.; Xue, G. L.; Du, C. Q. *Eur. J. Inorg. Chem.* **2008**, 239–250. (b) Ma, C.; Wu, Y.; Zhang, J.; Xu, Y.; Tu, B.; Zhou, Y.; Fang, M.; Liu, H. K. *CrystEngComm* **2012**, *14*, 5166–5169.